

CONF-980657-
To be presented at the 5th International Conference on Trends in Welding Research, June 1-5, 1998, Pine Mountain, Georgia

RECEIVED
AUG 13 1998
OSTI

**Neural Network Model for Predicting Ferrite Number
in Stainless Steel Welds**

J. M. Vitek, Y. S. Iskander, E. M. Oblow, S. S. Babu and S. A. David
Oak Ridge National Laboratory
Oak Ridge, Tennessee 37830-6376
U. S. A.

OSTI **MASTER**

DISTRIBUTION OF THIS DOCUMENT IS UNLIMITED

"The submitted manuscript has been authored by a contractor of the U. S. Government under contract No. DE-AC05-96OR22464. Accordingly, the U.S. Government retains a nonexclusive, royalty-free license to publish or reproduce the published form of this contribution, or allow others to do so, for U.S. Government purposes."

Abstract

Predicting the ferrite content in stainless steel welds is desirable in order to assess an alloy's susceptibility to hot cracking and to estimate the as-welded properties. Several methods have been used over the years to estimate the ferrite content as a function of the alloy composition. A new technique is described which uses a neural network analysis to determine the ferrite number. The network was trained on the same data set that was used to generate the WRC-1992 constitution diagram. The accuracy of the neural network predictions is compared to that for the WRC-1992 diagram as well as another recently proposed method. It was found that the neural network model was approximately 20% more accurate than either of the other two methods. In addition, it is suggested that further improvements to the neural network model, including the consideration of process variables, can be made which can lead to even better accuracy.

Introduction

The ferrite content in stainless steel welds and castings plays an important role in determining alloy properties and hot-cracking sensitivity. Mechanical properties as well as corrosion behavior are affected by the relative proportions of ferrite to austenite in the microstructure. In addition, weldability is strongly influenced by the ferrite content. The latter is affected by the mode of solidification, i.e., whether ferrite or austenite is the primary solidification phase. If the alloy undergoes primary austenite solidification during welding, minor elements such as sulfur can become quite enriched and lead to the stabilization of the liquid to lower temperatures, thereby significantly increasing the solidification range. This enrichment often increases the vulnerability of a weld to cracking during the final stages of solidification. In contrast, for primary ferrite solidification, segregation to the liquid of these minor tramp elements is kept to a minimum and hot-cracking sensitivity is reduced. During further cooling, in the solid state, the ferrite transforms to

austenite. This reaction is often incomplete under the cooling conditions prevalent during welding and, consequently, some residual ferrite is present at room temperature. Thus, the amount of ferrite that is present in the microstructure at room temperature is an indirect indication of the extent to which primary ferrite solidification took place and the degree to which ferrite transforms during cooling. Often, alloy specifications require a specific minimum level of ferrite as a means for assuring that primary ferrite solidification takes place in the alloy and that the alloy is resistant to hot cracking during welding.

Over the years there have been many attempts at devising a means of predicting ferrite content as a function of alloy composition. Constitution diagrams have been developed that convert the alloy composition into two factors, a chromium equivalent (Cr_{eq}) and a nickel equivalent (Ni_{eq}). The former contains alloying elements that influence the microstructure much like chromium, i.e., they are ferrite stabilizers, while the latter contains elements that behave like nickel, i.e., austenite stabilizers. These constitution diagrams plot ferrite levels as a function of these chromium and nickel equivalents. The first such diagram that was used for welding is the Schaeffler diagram¹. Since the introduction of the Schaeffler diagram, several modifications and improvements have been proposed²⁻⁷. Corresponding constitution diagrams for stainless steel castings have also been proposed^{8,9}. The various versions of constitution diagrams differ primarily in the coefficients that are used to convert alloy composition into the Cr_{eq} and Ni_{eq} . The most recent version of the constitution diagrams is the WRC-1992 diagram⁶. The equations for the Cr_{eq} and Ni_{eq} factors in the WRC-1992 diagram are:

$$Cr_{eq} = Cr + Mo + 0.7 Nb \quad (1a)$$

$$Ni_{eq} = Ni + 35 C + 20 N + 0.25 Cu \quad (1b)$$

where the elemental symbols represent the weight percent of each element.

Recently, another approach (Function Fit model) has been

DISCLAIMER

This report was prepared as an account of work sponsored by an agency of the United States Government. Neither the United States Government nor any agency thereof, nor any of their employees, makes any warranty, express or implied, or assumes any legal liability or responsibility for the accuracy, completeness, or usefulness of any information, apparatus, product, or process disclosed, or represents that its use would not infringe privately owned rights. Reference herein to any specific commercial product, process, or service by trade name, trademark, manufacturer, or otherwise does not necessarily constitute or imply its endorsement, recommendation, or favoring by the United States Government or any agency thereof. The views and opinions of authors expressed herein do not necessarily state or reflect those of the United States Government or any agency thereof.

DISCLAIMER

Portions of this document may be illegible in electronic image products. Images are produced from the best available original document.

proposed for predicting ferrite number in stainless steel weldments¹⁰. In this method, the difference in free energy between ferrite and austenite was calculated as a function of composition and this was related to the ferrite number. A regression analysis was used to determine the coefficients associating the ferrite number with the free energy change. It was found that this approach was comparable in accuracy to that of the WRC-1992 diagram. The advantage of this new approach was that certain restrictions with regard to the alloying elements that are considered, and their composition ranges, were eased¹⁰.

The ferrite content at room temperature is controlled by several factors and is a result of a series of microstructural transformations. The ferrite content is initially influenced by the solidification mode. This is determined by the alloy composition as well as the solidification conditions. Many investigations have shown that under rapid cooling conditions, alloys that would normally solidify in the primary ferrite mode instead solidify in the primary austenite mode¹¹⁻¹⁷. Once solidified, the alloy may undergo a solid state transformation of ferrite to austenite as the ferrite stability relative to austenite decreases with decreasing temperature, at least in the elevated temperature range of 800°C and higher. The extent of this transformation depends on the nucleation and diffusion-controlled growth of austenite. As in the case of the solidification mode, this transformation is strongly influenced by several factors, including the cooling rate, the degree of segregation within the ferrite phase, and the amount of austenite already present after solidification. Thus, the overall relationship between composition and ferrite content can be expected to be quite complicated. Simple relationships such as those in Eq. 1 cannot be expected to take into account all of the critical factors. Furthermore, constitution diagrams that rely on simple linear expressions for the Cr_{eq} and Ni_{eq} factors ignore interactions between the elements. For example, the influence of manganese levels on ferrite content may vary depending on the chromium, nickel or carbon content. Since the coefficients are constant over the entire composition range, such interactions are ignored in traditional constitution diagrams.

Therefore, it is desirable and appropriate to describe the residual ferrite in a more flexible manner, so that elemental interactions as well as process conditions can be factored into the relationships and, presumably, more accurate predictions would follow. Neural networks are ideally suited to improve the flexibility, robustness, and accuracy of ferrite predictions because they make use of non-linear regression methods. The inclusion of a variety of additional factors, such as cooling rate during welding, is straightforward. Furthermore, neural networks are able to develop relationships between variables that are otherwise difficult or impossible to identify by standard regression analyses. This paper describes the development of a neural network model for the prediction of ferrite content in stainless steel welds as a function of alloy composition. The well-known influence of processing conditions has not been considered; this feature will be addressed in future work.

Neural Network Development

A very simple description of the concept behind neural networks is given below. There is extensive literature on the theory behind neural networks. The reader is referred to other publications for more details¹⁸⁻¹⁹. Neural networks are modeled after the learning process in the human brain. A network structure consists of interconnected layers of nodes; the nodes include input and output nodes as well as internal, hidden nodes. These nodes are "connected" to each other so that the value of one node will affect the value of another. The relative influence that a given node has on another one is specified by the "weight" that is assigned to each connection. A schematic diagram of a simple neural network is shown in Figure 1. There are three layers in the

Output Layer

Hidden Layer

Input Layer

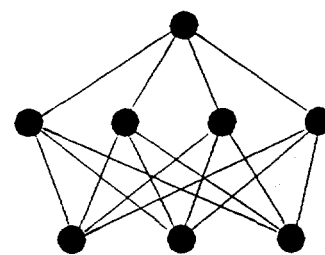


Figure 1: Schematic diagram showing the multiple layer structure of a neural network and the inter-connectivity between the nodes of the network.

diagram. In the example of Figure 1, the input layer has three nodes, representing three input variables such as chromium, nickel and carbon concentration. The output layer contains one node, corresponding to one output variable such as ferrite number. In addition, one hidden layer with four nodes is shown in the diagram. The neural network is trained by introducing a training data set containing experimental data for inputs and corresponding outputs. A training routine is then carried out in which outputs are predicted and these are compared with the true outputs. Starting with a simple initial configuration, the weights are continuously adjusted by an optimization process to yield better, more accurate predictions. The first task is to identify the network architecture, including the input and output variables and the optimum number of hidden nodes. Once this is determined, then the learning process, which consists of hundreds of thousands of iterations, develops the complicated set of empirical relationships between the input and output variables. There is minimal influence from the user while the network "learns" how to associate the outputs to the inputs with a minimum error. In the present study, commercially available software (NeuralWorks Professional II/PLUSTM 20) was used for the neural network analysis. A feed-forward network with a back propagation learning scheme was utilized. A sigmoidal transfer function was used to convert the weighted input to a node to an output value from the node.

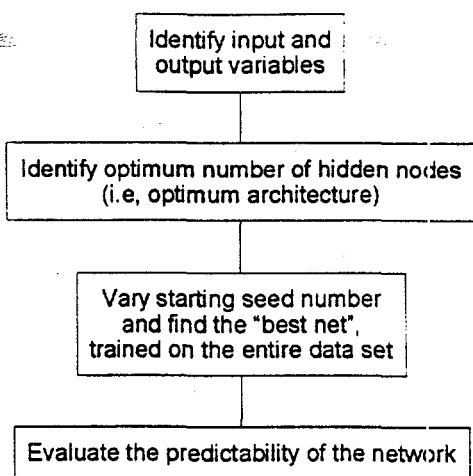


Figure 2: Flow chart showing the sequence of operations to identify the optimum network architecture and to train the best network.

The analysis scheme to develop the final neural network for ferrite number prediction is summarized in Figure 2. The optimum architecture was identified by using different combinations of learning and test subsets of the entire data set. Only a single hidden layer configuration was examined. It was found that as the number of hidden nodes increased from one to five, the errors in both the ability of the network to match the learning data ("learnability") and to predict the ferrite number for new data ("predictability") decreased. Beyond five hidden nodes, the network errors for both factors did not change significantly. Normally, as the number of hidden nodes increases, the learnability of the network improves continuously while the predictability reaches a peak and then deteriorates. It is believed that the behavior found in the current study, where both the predictability and learnability reach plateaus, can be traced to the scatter in the experimental data, and the inherent inconsistencies due to the accuracy of the chemical analyses and the variations in ferrite number measurements from laboratory to laboratory. Therefore, five hidden nodes were used for the optimum architecture since this represented the smallest number of nodes that still achieved the best learnability and predictability.

Once the optimum architecture was identified, then the "best" network was found by teaching the network on the entire experimental data set. Numerous initial seed numbers that define the initial weight configuration were tested²¹. By learning with several different starting weight distributions, a final network with a minimum error in predicting the ferrite number for the entire data set was found.

An attempt was made at quantifying the predictability of the final network that was developed. This was done by removing, at random, 10 points from the entire data set of 961 points and training a network with the same optimum architecture and initial seed number on the remaining 951 points. The resultant network

was tested on the removed data. This was repeated for ten different combinations of training and testing data. The error in predicting the FN under these conditions is a reasonable estimate of the error that can be expected when the network is applied to new, previously unseen data.

Experimental Ferrite Number Data

The same data that were used in the development of the WRC-1992 constitution diagram⁶ and the more recent Function Fit model¹⁰ were used in this study. The data consist of three compilations of composition and measured ferrite number (FN)^{22,24}. As with the conventional constitution diagrams, ferrite number has been used as an indicator of the ferrite content. There are many advantages to using this quantity rather than a measurement of the actual volume percent of ferrite in the microstructure²⁵. The data consisted of FN measurements made by various laboratories on welds made with a variety of arc welding techniques. For this study, no attempt was made to include the welding process as an input variable. Nonetheless, it is likely that the welding process has a significant effect on the ferrite content and this effect will be considered in a later investigation.

Since the experimental data came from several different sources, the composition analyses did not always include the same elements. Therefore, it was decided to consider only those elements for which a chemical analysis was available for all the data. Consequently, eight input nodes were used, corresponding to the weight percent concentrations of eight elements: Cr, Ni, Mn, C, N, Mo, Si, and Fe. The eighth input variable, the Fe concentration, was calculated as the remaining balance in the chemical analysis, taking account of all of the elements that were analyzed and not just the seven common elements listed above. Other elements such as Nb, Cu, and Ti, that have been included in the calculation of chromium and nickel equivalent factors in the literature (e.g., see Eq. 1) and are likely to have an impact on the ferrite number, were ignored because their concentrations were not known in all cases. The omission of potentially important input variables (e.g. other elements) has the same effect as introducing stochasticity into the experimental FN data. This produces some unavoidable scatter and limits the network's ability to fit the data. However, with the currently developed neural network as a basis, the addition of other elements as input variables can be made and this is planned for work in the future.

By using data from various sources, it is likely that some data were more reliable than others^{22,23}. However, no attempt was made to screen the data in advance, or to exclude data in any way. Naturally, this practice of using all the data meant that considerable scatter in the training data was present. Often, data points with basically identical compositions had significantly different measured FN values. Some of this may be attributable to different welding processes that were used, but much of the variability is unavoidable and is due to variations from laboratory to laboratory in chemical analysis and in FN measurement.

Results

A plot of the experimental FN versus the predicted FN for the neural network model is shown in Figure 3a. For comparison, similar plots for the WRC-1992 constitution diagram⁶ and Function Fit model¹⁰ are shown in Figures 3b and 3c, respectively. The straight lines represent exact agreement between the predicted and measured FN values. The WRC-1992 predictions for the data were calculated using an interpolation program based on the published diagram²⁶. At first glance, the three diagrams are comparable. In Figure 3d, the neural network model

predictions and the WRC-1992 predictions are superimposed. It can be seen that for most of the data, the two methods yield similar FN values. However, in several cases, the WRC-1992 predictions are significantly worse than those of the neural network model. These data have been highlighted with straight arrows. The WRC-1992 predictions for these selected points both underestimate and overestimate the measured values and their error can be as much as 20 FN worse than the error in the neural network model. In only one case (curved arrow, Figure 3d) is the neural network model prediction significantly worse than the WRC-1992 prediction.

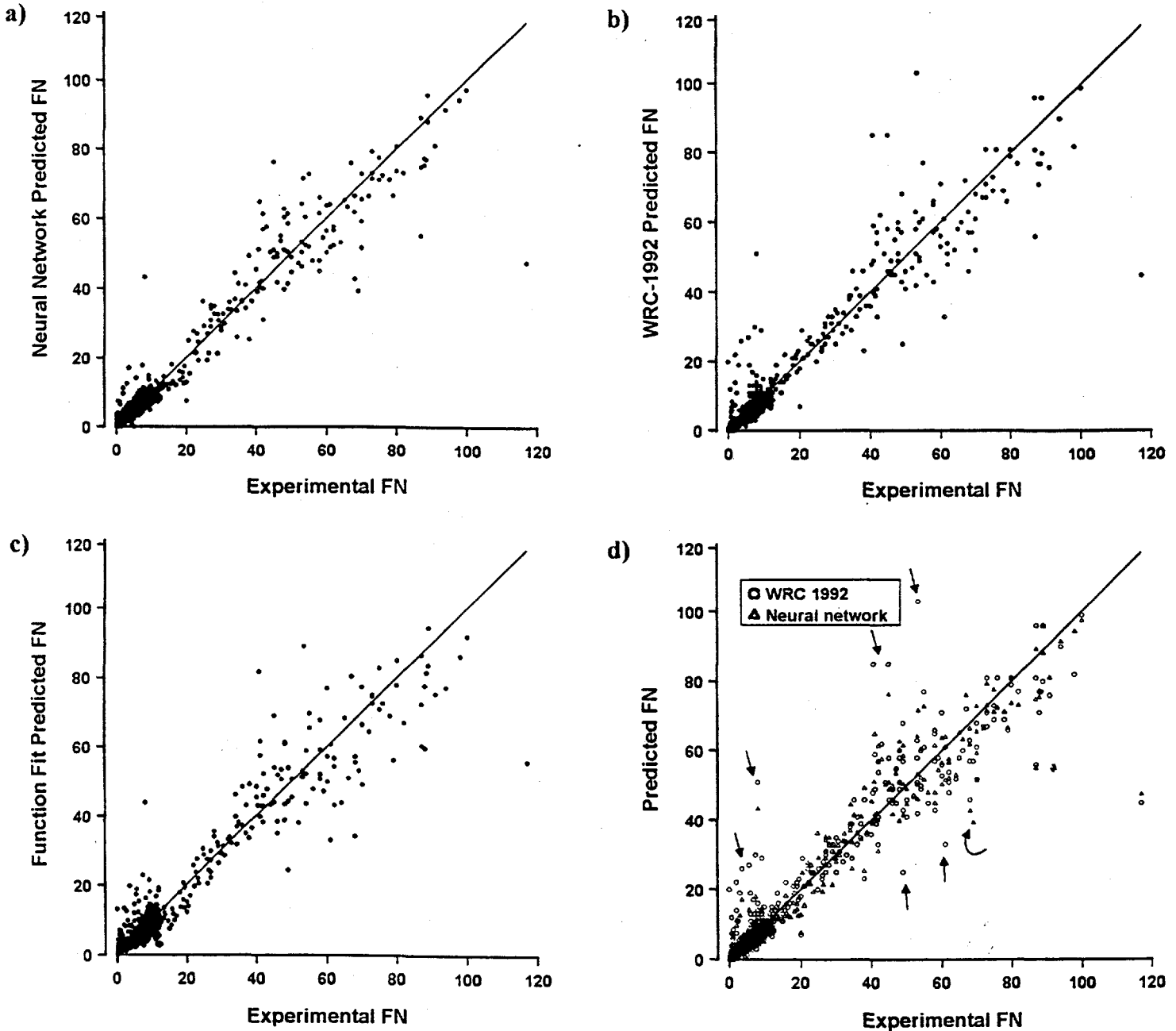


Figure 3: Experimentally measured FN versus predicted FN for (a) neural network model, (b) WRC-1992 constitution diagram, and (c) Function Fit model. The plots in (a) and (b) are superimposed in (d) for easy comparison. The significance of the arrows in (d) is explained in the text.

The root mean square errors between the measured and predicted FN values for the three methods are compared in Table 1. While the Function Fit model and WRC-1992 diagram accuracies are comparable, the neural network model developed in this study is significantly better, with a root mean square error decrease of approximately 20%. The accuracies of the three approaches are compared pictorially in Figure 4, where histograms showing the frequency distribution of errors are plotted. The point beyond 20 represents the sum of all errors greater than 20 FN. Once again the present neural network model shows the best behavior. The distribution for the neural network model is less spread out than in the other two models, and the number of prediction errors greater than 20 FN (8) is roughly half of the corresponding numbers for the WRC-1992 diagram (17) and the Function Fit model (15).

Table 1: Comparison of Root Mean Square Errors for Three FN Prediction Methods

Prediction Method	Root Mean Square Error
WRC-1992	5.8
Function Fit Model	5.6
Neural Network Model	4.8

As described in an earlier section, an attempt was made at assessing the predictability of the neural network model by training the network with only 99% of the data and then predicting the FN for the "unseen" 1% of the data. This was done with ten different 99%-1% combinations. This method of assessing the predictability is a truer measure than simply the root mean square error over all the data (Table 1) since it is based on data not previously seen by the model. The average root mean square error for the predictions on these ten sets of new data was 4.6, which is basically equivalent to the overall root mean square error for the neural network trained and tested and the entire data set (Table 1). Corresponding prediction accuracy values for the WRC-1992 and the Function Fit models are not available for

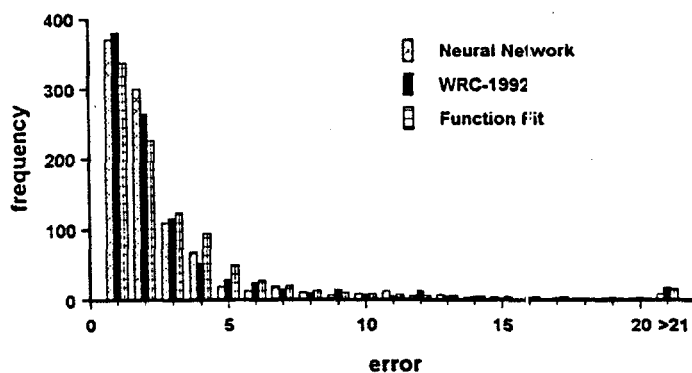


Figure 4: Prediction error histograms showing frequency distribution of errors for the three prediction methods.

comparison. Nonetheless, it is concluded that the accuracies quoted in Table 1, which represent the degree to which the three models reproduce or "fit" the known data, are also reasonable estimates of the accuracies of the three models for predicting FN for new data.

Discussion

When comparing the present neural network model for ferrite number prediction with the WRC-1992 diagram, it should be noted that the WRC-1992 diagram has a quoted upper limit for the Ni_{eq} of 17. No attempt was made in the present study to separate out the experimental data which had an Ni_{eq} greater than 17. In the entire experimental data set of 961 points, there were 89 measurements on alloy compositions with $Ni_{eq} > 17$. The root mean square error of the WRC-1992 predictions for these 89 measurements was calculated and found to be essentially the same as for the entire data set (5.9 versus 5.8, respectively). Thus, inclusion of all the data when comparing the WRC-1992 predictions with the neural network model did not introduce any appreciable increase in the calculated errors.

The neural network model for ferrite number prediction was found to be more accurate than the other two methods that were examined (see Table 1). While this is certainly an encouraging result, the neural network approach has the potential for being even better. As noted earlier, only those elements which were chemically analyzed in all the data were considered in the neural network model. Among the elements that were not included, several are known to have an influence on the ferrite number. Nb and Cu were not considered and these elements are included in the coefficients in the WRC-1992 diagram⁶ (see Eq. 1). In addition, Ti, V, and Co were not considered and these elements have also been suggested as terms for chromium and nickel equivalents by various authors⁷. A preliminary check of the neural network predictions with the largest errors ($\Delta FN \sim 6$ or larger) indicated that in most cases the concentrations of some of the omitted elements were significant. Thus, it can be expected that significant improvements in the prediction accuracy can be achieved with the addition of these neglected elements.

The use of neural networks for predicting ferrite number has an additional advantage in that process variables can be included as well as composition as inputs to the model. For example, many studies have shown that at high cooling rates prevalent during laser welding or electron beam welding the residual ferrite content can be significantly different than that found for the same alloy under typical arc welding conditions¹¹⁻¹⁷. The dramatic changes in ferrite content are often attributable to a change in the solidification mode so that an alloy that solidifies in the primary ferrite mode under near-equilibrium conditions can change to primary austenite solidification when rapidly cooled. In theory, this additional factor that influences ferrite number can be incorporated into the neural network model. Such an enhancement is planned for future work.

The neural network model cannot be condensed into a simple pictorial form such as the WRC-1992 diagram. Thus, the variation in ferrite number with composition cannot be viewed

directly. In fact, the complicated interactions among the elemental concentrations in the neural network model are difficult to describe in a qualitative manner and in this way a physical interpretation of the influence of the various elements is missing. However, the neural network model can be condensed into an analytical form for easy use. Details describing such an analytical form may be found elsewhere²¹. With the use of an analytical expression for ferrite number as a function of composition, determination of ferrite number can be easy, convenient, accurate, and essentially instantaneous. Interpolation, as required with the use of the WRC-1992 diagram, is unnecessary. Furthermore, the variation in ferrite number as a function of a given element concentration can be readily calculated, thereby providing a description of the effect that such an element has on the ferrite level. The current model is available for use at the following world wide web site: "http://engm01.ms.ornl.gov".

Finally, it is interesting to speculate on other applications of neural network models beyond simply ferrite number prediction. Ultimately, ferrite number prediction is a means to an end, namely the prediction of an alloy's susceptibility to weld cracking and even the alloy's mechanical properties and corrosion resistance. In this regard, it may be possible to use neural networks to directly correlate composition with these properties and bypass the ferrite number stage completely. Neural networks are ideally suited for such applications. Several neural network models have already been developed to predict weld alloy properties^{27,28}. The only impediment for using neural network models to predict properties of stainless steels directly is the availability of a sufficiently complete database. If such a database were available, development of the required neural network models could easily follow and the use of constitution diagrams and ferrite numbers could be bypassed altogether.

Summary and Conclusions

A neural network model for prediction of ferrite number in stainless steels has been developed. The neural network was trained on the same data that were used to develop the WRC-1992 constitution diagram. The model uses the concentration of Fe, Cr, Ni, C, N, Mn, Mo, and Si as inputs. The accuracy of the neural network model was compared with that of the WRC-1992 constitution diagram as well as a recently developed alternative Function Fit model. It was found that over the entire data set, the neural network model predictions were approximately 20% better than either of the two alternatives. With the inclusion of additional elements into the model, such as Nb, Cu, and Ti, it is expected that the predictive accuracy can be improved still further. In addition, work is underway to incorporate process variables into the model to account for the effect of high cooling rate on ferrite content.

Acknowledgments

This research was sponsored by the Division of Materials Sciences, U. S. Department of Energy, under contract number DE-AC05-96OR22464 with Lockheed Martin Energy Research

Corporation. The authors would also like thank Drs. C. W. Glover, G. M. Goodwin, and Q. Han for fruitful discussions and review of the paper.

References

1. A. Schaeffler, *Metal Progress*, 56, 680-680B (1949).
2. F. C. Hull, *Weld. J.*, 52, 193s-203s (1973).
3. W. T. DeLong, *Weld. J.*, 53, 273s-286s (1974).
4. N. I. Kakhovskii, V. N. Lipodaev, and G. V. Fadeeva, *Avt. Svarka*, 5, 55-57 (1980).
5. T. A. Siewert, C. N. McCowan, and D. L. Olson, *Weld. J.*, 67, 289s-298s (1988).
6. D. J. Kotecki and T. A. Siewert, *Weld. J.*, 71, 171s-178s (1992).
7. D. L. Olson, *Weld. J.*, 64, 281s-295s (1985).
8. H. Schneider, *Foundry Trade J.*, 108, 562-563 (1960).
9. E. A. Schoefer, *Weld. J.*, 53, 10s - 12s, (1974).
10. S. S. Babu, J. M. Vitek, Y. S. Iskander and S. A. David, *Sci. and Technol. Weld. Joining*, 2(6), 279-285 (1997).
11. J. M. Vitek, A. DasGupta, and S. A. David, *Metall. Trans.*, 14A, 1833-1841 (1983).
12. S. Katayama and A. Matsunawa, Proc. of ICALEO 84, Boston, Massachusetts, 44, 60-67 (1984).
13. S. A. David, J. M. Vitek, and T. L. Hebble, *Weld. J.*, 66, 289s-300s (1987).
14. M. Bobadilla, J. Lacaze, and G. Lesoult, *J. Cryst. Growth*, 89, 531- (1988).
15. J. W. Elmer, S. M. Allen, and T. W. Eagar, *Metall. Trans. A*, 20A, 2117-2131 (1989).
16. J. C. Lippold, *Weld. J.*, 73, 129s-139s (1994).
17. T. Koseki and M. C. Flemings, *Metall. Mater. Trans. A*, 28A, 2385-2395 (1997).
18. D. E. Rumelhart, B. Widrow and M. A. Lehr, *Comm ACM*, 37, 87-92 (1994).
19. C. M. Bishop, *Rev Sci Instr.*, 65, 1803-1832 (1994).
20. NeuralWare, Inc., Pittsburgh, Pennsylvania (1995).
21. J. M. Vitek, Y. S. Iskander and E. M. Oblow, to be published.
22. D. J. Kotecki, *Weld. J.*, 65, 273s-278s (1986).
23. D. J. Kotecki, *Weld. J.*, 68, 431s-441s (1989).
24. C. N. McCowan, T. A. Siewert, and D. L. Olson, *WRC Bulletin*, 343 (1989).
25. D. J. Kotecki, *Weld. J.*, 76, 24s-37s (1997).
26. F. B. Lake, ESAB Welding and Cutting Products, Hanover, Pennsylvania.
27. B. Chan, M. Bibby, and N. Holtz, *Canad. Metall. Quart.*, 34, 353-356 (1995).
28. T. Cool, H. K. D. H. Bhadeshia, and D. J. C. MacKay, *Mater. Sci. Eng'g.*, A223, 186-200 (1997).